The static quark potential from the gauge invariant Abelian decomposition

Nigel Cundy [a,*], Y.M. Cho [b,c], Weonjong Lee [a], Jaehoon Leem [a]

[a] *Lattice Gauge Theory Research Center, FPRD, and CTP, Department of Physics and Astronomy, Seoul National University, Seoul, 151-747, South Korea*
[b] *Administration Building 310-4, Konkuk University, Seoul, 143-701, South Korea*
[c] *Department of Physics & Astronomy, Seoul National University, Seoul, 151-747, South Korea*

ABSTRACT

We investigate the relationship between colour confinement and topological structures derived from the gauge invariant Abelian (Cho–Duan–Ge) decomposition. This Abelian decomposition is made imposing an isometry on a colour field n which selects the Abelian direction; the principle novelty of our study is that we have defined this field in terms of the eigenvectors of the Wilson loop. This allows us to establish an equivalence between the path ordered integral of the non-Abelian gauge fields with an integral over an Abelian restricted gauge field which is tractable both theoretically and numerically in lattice QCD. By using Stokes' theorem, we can relate the Wilson loop in terms of a surface integral over a restricted field strength, and show that the restricted field strength may be dominated by topological structures, which occur when one of the parameters parametrising the colour field n winds itself around a non-analyticity in the colour field. If they exist, these objects will lead to an area law scaling for the Wilson loop and provide a mechanism for quark confinement. We search for these structures in quenched lattice QCD. We perform the Abelian decomposition, and find that the restricted field strength is dominated by peaks on the lattice. Wilson loops containing these peaks show a stronger area-Law and thus provide the dominant contribution to the string tension.

1. Introduction

Colour confinement in QCD is one of the outstanding problems in physics. Although several possible confinement mechanisms have been proposed (for example, Abelian dominance [1,2] or monopole condensation [3–7]), none have been convincingly demonstrated to be correct. However, there has been important recent progress. Using a gauge invariant Abelian decomposition (the Cho–Duan–Ge (CDG) decomposition) and introducing the concept of the C-projection similar to the GSO-projection in string theory, Cho (and collaborators) have shown how to calculate the one-loop effective action of QCD gauge-invariantly and demonstrated that the effective potential condenses the monopole liquid [8], implying that monopole condensation drives confinement. This project (of which this Letter is the start) aims to verify and expand on this result in lattice QCD.

Lattice QCD has demonstrated the linear confining potential, but it has not been so successful determining what causes confinement. A popular mechanism studied in lattice QCD is Abelian dominance proposed by 't Hooft, which asserts that only the Abelian

(i.e., neutral) part of QCD causes confinement [9]. This makes intuitive sense, since the coloured part of QCD is confined. It has been studied on the lattice by decomposing the QCD potential into colour-neutral and coloured parts, using a gauge condition, such as the Maximal Abelian Gauge (MAG) or Laplacian Abelian Gauge to separate the Abelian part [10–13]. Similar approaches have been used to study monopole condensation in lattice QCD [14,15].

This approach has serious defects. The whole process is centred around fixing to one particular gauge, so it does not demonstrate a gauge-invariant confinement mechanism. It also does not indicate what confines the colour. If an Abelian potential alone is enough for colour confinement, we ought to have confinement in the Abelian QED.

However, the gauge invariant CDG decomposition (also referred to as the Cho–Faddeev–Niemi decomposition) avoids such defects [16–20]. Unlike the more popular MAG, this decomposition splits the QCD potential into the restricted (neutral) part and the valence (coloured) part gauge invariantly. It also separates the topological part of the Abelian part of the gauge field. This decomposition can be used for a gauge-invariant investigation of the topological basis of confinement.

Consider SU(2) QCD, and select a normalised ($n^a n^a = 1$) Abelian direction $n \equiv \lambda^a n^a$, where λ represents a Pauli matrix (or Gell-Mann

* Corresponding author.

matrix in higher gauge groups). To construct the Abelian decomposition, we impose the isometry condition on A_μ to obtain the restricted potential $\hat{A}_\mu$

$$D_\mu[\hat{A}]n = 0, \qquad A_\mu^a \to \hat{A}_\mu^a = \mathcal{B}_\mu^a + \mathcal{C}_\mu^a,$$
$$\mathcal{B}_\mu^a = \frac{1}{2}n^a A_\mu^b n^b, \qquad \mathcal{C}_\mu^a = \frac{i}{2g}\epsilon^{abc}n^b \partial_\mu n^c. \qquad (1)$$

The CDG decomposition arises by adding the valence potential $X_\mu = A_\mu - \hat{A}_\mu$ to the restricted potential

$$A_\mu = \hat{A}_\mu + X_\mu = \mathcal{B}_\mu + \mathcal{C}_\mu + X_\mu, \qquad \mathrm{tr}(nX_\mu) = 0. \qquad (2)$$

The decomposition has several important features [16,17]: Firstly, the restricted potential, despite being reduced, retains the full non-Abelian gauge degrees of freedom. Secondly, the valence potential transforms gauge covariantly: it represents the gauge covariant coloured gluons. Thirdly, the decomposition is gauge invariant. Once the Abelian direction n is chosen, the decomposition follows automatically regardless of the choice of gauge.

But most importantly, the decomposition separates the topological potential gauge independently. The restricted potential $\hat{A}_\mu$ is made of two parts, the naive Abelian potential $\mathcal{B}_\mu$ and the topological potential $\mathcal{C}_\mu$, which can describe the Wu–Yang monopole [21] when n has an isolated point singularity representing the monopole topology $\pi_2(S^2)$ [16,17]; this monopole structure is invariant under infinitesimal and analytic gauge transformations.

We aim (eventually) to identify the cause of confinement by examining the topological structures contained within a suitably chosen Abelian direction n and their effects on the corresponding restricted field strength. The purpose of this initial Letter is to demonstrate the feasibility of our approach, to isolate the topological potential and to suggest that it dominates the confining string. Later studies will further examine the consequences of this construction. We aim to confirm whether the topological structures in the restricted gauge field strength $\hat{F}_{\mu\nu}[\hat{A}]$ which, if they exist, might drive confinement can be associated with isolated monopoles, a condensed monopole/anti-monopole liquid, or some other topological structures.

To construct the Abelian decomposition on the lattice, we must first choose the $N_C - 1$ Abelian directions n_j, built from a $SU(N_C)$ matrix θ, so $n_3 = \theta\lambda^3\theta^\dagger$ (N_C is the number of colours, the subscript 3 indicates that n_3 is constructed from the third Gell-Mann matrix). There are different ways of selecting θ, including $\theta \in SU(N_C)/(SU(N_C - 1) \times U(1))$ and $\theta \in SU(N_C)/(U(1))^{N_C-1}$. Choosing $\theta \in SU(N_C)/(U(1))^{N_C-1}$ is advantageous as it contains all the possible Abelian directions. It is important to select this θ so all these configurations contribute to confinement [16].

In this Letter we observe that we can always choose θ so that the static quark potential for the restricted field is identical to that of the full gauge field.[1] *We note that there always exists a $SU(N_C)/(U(1))^{N_c-1}$ field θ which diagonalises the gauge links and removes the path ordering of the Wilson loop, an observable used to measure the static potential.* By choosing the Abelian direction judiciously, we can always avoid the complicated path ordering in the Wilson loop and reduce it to an Abelian form: we can always make the contribution of the valence potential X_μ to the Wilson loop vanish. This is natural: X_μ describes the coloured gluons and cannot play any role in confinement. This is Abelian dominance,

which has been demonstrated theoretically [9]. But to show it by explicitly choosing a particular Abelian direction is really remarkable.

Having thus selected n, we implement the isometry condition (1) on the lattice and construct the restricted field consistently, which allows us to express the Wilson loop in terms of a surface integral over the restricted gauge field strength tensor. Our relationship for the string tension in terms of this restricted field is exact: we do not require any approximations or additional path integrals. We perform the lattice CDG decomposition, isolate the restricted potential $\hat{A}_\mu$ and the topological potential $\mathcal{C}_\mu$ and search for the topological structures in the restricted field strength, finding that they may cause an area law behaviour of the Wilson loop. We outline how these topological structures arise in SU(2), leaving a fuller description and the extension to higher gauge groups to a subsequent work. If these structures exist (we do not prove in the theoretical analysis here that configurations containing them will contribute in practice) they will provide a mechanism for quark confinement.

By calculating the Wilson loop in a pure Yang Mills SU(3) lattice gauge theory with the full potential A_μ, the restricted potential $\hat{A}_\mu$, and the topological potential $\mathcal{C}_\mu$, we pinpoint which potential generates the confining area law and is thus responsible for confinement. In this initial calculation, we concentrate on the string tension and an examination of the component of the restricted field responsible for confinement. Our result suggests that confinement is caused by the topological potential.

Similar lattice calculations, by the Chiba-KEK Lattice Group led by Kondo [22–24], have recently used the gauge independent Abelian decomposition to provide evidence for monopole dominance in the confining potential. As far as we know, these are the first gauge invariant lattice calculations to suggest monopole dominance in the confining potential. The most important difference between their work and ours is that they use a different choice of n whose θ is taken from a different subgroup of SU(3). These calculations, however, have unsatisfactory features. Firstly, their relationship between the Wilson loop and the restricted field (based on [25,26]) requires a path integral over all possible θ, in effect enlarging the gauge group by introducing a new SU(3)/U(2) dynamical field. They then fixed θ (restoring the gauge group to SU(3)) by imposing the condition $[n, D^2[A]n] = 0$, which breaks the relationship between the Wilson loops of the restricted and original gauge fields. Secondly, they have chosen the 'minimal' Abelian configuration for n which leaves $SU(3)/(SU(2) \times U(1))$ invariant, choosing n as only the λ^8-like Abelian direction, neglecting any contribution from the second Abelian direction constructed from λ^3. Clearly this n can not describe the most general SU(3) Abelian topologies. In this sense their monopole dominance is incomplete.

Here we construct the Abelian decomposition by rigorously imposing the isometry (1), choosing an Abelian direction n which covers all possible SU(3) topological structures, and gives an exact equivalence between the Wilson loops of the restricted and original gauge fields. This novel feature of our Letter not only re-enforces the topological dominance but also makes it more precise. We will search for evidence of monopole condensation or some other mechanism in future work.

The Letter is organised as follows. In Section 2 we discuss the Abelian decomposition and its relation to the Wilson loop and thus the static quark potential. In Section 3 we discuss how topological structures which generate confinement may arise in this construction. We present numerical evidence in Section 4. We conclude in Section 5. Early results were presented in [27,28].

---

[1] In practice, a different n should be selected for each Wilson loop to ensure that the restricted field can account for the confining potential. In this initial work, to save computer time, we use a single choice of n for all our Wilson loops, meaning that the link between the static potential of restricted and full QCD is inexact. Simulations without this simplification will be presented in a future work.

2. Abelian decomposition and Stokes' theorem

We use the convention that the superscript a on a Gell-Mann matrix, λ^a, implies that it should be summed over all values of a ($\lambda^a A^a \equiv \sum_{a=1}^{N_C^2-1} \lambda^a A^a$), while the index j is restricted only to the diagonal Gell-Mann matrices (in the standard representation $A^j \lambda^j \equiv \sum_{j=3,8,\ldots,N_C^2-1} \lambda^j A^j$). The Wilson loop, W_L, measures the confining potential in a theory with a SU(N_C) gauge field, $A_\mu = \frac{1}{2} A_\mu^a \lambda^a$ [29],

$$W_L[C_s] = \frac{\operatorname{tr} W[C_s]}{N_C}, \qquad W[C_s] = \mathcal{P}\left[e^{-ig \oint_{C_s} dx_\mu A_\mu(x)}\right]. \tag{3}$$

C_s is a closed curve of length L which starts and finishes at a position s and $\mathcal{P}$ represents path ordering. It is expected that the vacuum expectation value of the Wilson loop should scale as $\langle W_L[C_s]\rangle \sim e^{-\rho \Sigma}$, where Σ is the area of the surface enclosed by the curve C_s and ρ is the string tension. We only consider planar Wilson loops: C_s is a rectangle of temporal extent T and spatial extent R (we will later restrict ourselves to loops in the xt plane). The static quark potential is given by $V(R) = -\lim_{T\to\infty} \log(\langle W_L[C_s]\rangle)/T$. A linearly rising $V(R)$ is a signal for confinement [29].

To define the path ordering, we split C_s into infinitesimal segments of length $\delta\sigma$, with the gauge link $U_\sigma \in$ SU(N_C) $= \mathcal{P}[e^{-ig\int_\sigma^{\sigma+\delta\sigma} A_\sigma d\sigma}] \sim e^{-ig\delta\sigma A_\sigma}$, $0 \leqslant \sigma \leqslant L$ represents the position along the curve and $A_\sigma \equiv A_{\mu(\sigma)}(x(\sigma))$. We have assumed and will require throughout this work that the gauge field is differentiable. This limits us to continuous gauge transformations (formed by repeatedly applying $A_\mu \to A_\mu + \frac{1}{g}\partial_\mu\alpha + i[A_\mu,\alpha]$ for infinitesimal and differentiable $\alpha \equiv \frac{1}{2}\alpha^a\lambda^a$). We also neglect the effects of the corners of the Wilson loop (rounding them as necessary to avoid a discontinuity as σ increases). This gives,

$$W[C_s] = \lim_{\delta\sigma\to 0} \prod_{\sigma=0,\delta\sigma,2\delta\sigma,\ldots}^{L-\delta\sigma} U_\sigma. \tag{4}$$

We introduce a field $\theta_\sigma \equiv \theta(x(\sigma)) \in U(N_C)$ and insert the identity operator $\theta_\sigma\theta_\sigma^\dagger$ between each pair of neighbouring gauge links on C_s. θ is chosen so that $\theta_\sigma^\dagger U_\sigma\theta_{\sigma+\delta\sigma}$ is diagonal.[2] θ_s therefore contains the eigenvectors of $W[C_s]$ (the index s indicates that θ_s refers to the field at the location where the Wilson loop starts and ends). As the phases of the eigenvectors are arbitrary, this definition only determines θ up to a $(U(1))^{N_C}$ transformation $\theta \to \theta\chi$. No physical observable depends on χ, but in practice it is useful to select the phases and ordering of the eigenvectors by some arbitrary *fixing condition*, giving a unique choice of $\theta \in$ SU(N_C)/$(U(1))^{N_C-1}$. Under a gauge transformation, $U_\sigma \to \Lambda_\sigma U_\sigma \Lambda_{\sigma+\delta\sigma}^\dagger$ for $\Lambda = e^{i\alpha^a\lambda^a} \in$ SU(N_C), $\theta \to \Lambda\theta\chi$, where the $(U(1))^{N_C-1}$ factor χ depends on the fixing condition. With $\theta_\sigma^\dagger U_\sigma\theta_{\sigma+\delta\sigma} = e^{i\sum_{\lambda^j\mathrm{diagonal}} \delta\sigma \hat{u}^j\lambda^j}$ for real $\hat{u}$,

$$\theta_s^\dagger W[C_s]\theta_s = e^{i\sum_{j=3,8,\ldots}\lambda^j\oint_{C_s} d\sigma\,\hat{u}_\sigma^j}, \tag{5}$$

removing the non-Abelian structure and the path ordering.

We will apply Stokes' theorem to express W as a surface integral. First we extend the definition of θ and $\hat{u}^j$ across all space. For θ, we construct nested curves in the same plane as C_s and stack these curves on top of each other in the other dimensions. We define θ so it diagonalises each W constructed from one of these

curves. For $\hat{u}^j$, we construct a field $\hat{U}$ such that $\theta^\dagger(x)\hat{U}_\mu(x)\theta_{x+\delta\sigma\hat{\mu}}$ is diagonal $\forall x, \mu$ and $\hat{U}_\mu(x) = U_\mu(x)$ $\forall x, \mu \in C_s$. Thus

$$\left[\lambda^j, \theta_{\mu,x}^\dagger\hat{U}_{\mu,x}\theta_{x+\hat{\mu}\delta\sigma}\right] = 0, \tag{6}$$

$$\hat{U}_{\mu,x}n_{j,x+\delta\sigma\hat{\mu}}\hat{U}_{\mu,x}^\dagger - n_{j,x} = 0, \quad n_{j,x} \equiv \theta_x\lambda^j\theta_x^\dagger \tag{7}$$

are satisfied $\forall x, j$. Note that n_j is independent of the choice of χ. We relate $\hat{U}$ to the physical gauge field through a second field $\hat{X}$, defined by $U_\mu(x) = \hat{X}_\mu\hat{U}_\mu$. For later convenience (Eq. (12)), we impose the condition

$$\operatorname{tr}\left[n_{j,x}\left(\hat{X}_{\mu,x}^\dagger - \hat{X}_{\mu,x}\right)\right] = 0. \tag{8}$$

We choose the solution to Eqs. (7) and (8) which maximises $\operatorname{tr}(\hat{X})$, a condition which is both gauge invariant and satisfied along C_s where $\hat{U} = U$ and $\hat{X} = 1$. Under a gauge transformation, $n_x \to \Lambda_x n_x\Lambda_x^\dagger$, $\hat{U}_\mu(x) \to \Lambda_x\hat{U}_{\mu,x}\Lambda_{x+\hat{\mu}\delta\sigma}^\dagger$ and $\hat{X}_{\mu,x} \to \Lambda_x\hat{X}_{\mu,x}\Lambda_x^\dagger$, so Eqs. (7) and (8) are gauge-invariant. Eqs. (7) and (8) are lattice equivalents of the defining equations of the CDG decomposition [16,17,19,20,18], described in the continuum by the isometry condition (Eqs. (1) and (2))

$$A_\mu = \hat{A}_\mu + X_\mu, \qquad D_\mu[\hat{A}]n_j = 0,$$
$$D_\mu[\hat{A}]\alpha \equiv \partial_\mu\alpha - ig[\hat{A}_\mu,\alpha], \qquad \operatorname{tr}(n_j X_\mu) = 0,$$
$$\hat{A}_\mu = \frac{1}{2}\left[n_j\operatorname{tr}(n_j A_\mu) + \frac{i}{2g}[n_j,\partial_\mu n_j]\right], \tag{9}$$

with $U_\mu \sim e^{-i\delta\sigma A_\mu}$ and $\hat{X}_\mu \sim e^{-i\delta\sigma X_\mu}$ (to O($\delta\sigma^2$)).

We express $\hat{U}$ as $\hat{U}_{\mu,x} \equiv \theta_x e^{i\lambda^j\delta\sigma\hat{u}_{\mu,x}^j}\theta_{x+\hat{\mu}\delta\sigma}^\dagger$ for real $\hat{u}$. Since $\hat{U}_\mu(x) = U_\mu(x)$ $\forall x \in C_s$, $W[C_s,U] = W[C_s,\hat{U}] = \theta_s W[C_s,\theta^\dagger\hat{U}\theta]\theta_s^\dagger = \theta_s e^{i\lambda^j\oint_{C_s}\hat{u}_\sigma^j d\sigma}\theta_s^\dagger$. If $\hat{u}$ is differentiable, applying Stokes' theorem to this line integral gives

$$\theta_s^\dagger W[C_s]\theta_s = e^{i\lambda^j\int_{x\in\Sigma} d\Sigma_{\mu\nu}\,\hat{F}_{\mu\nu}^j}, \qquad \hat{F}_{\mu\nu}^j = \partial_\mu\hat{u}_\nu^j - \partial_\nu\hat{u}_\mu^j, \tag{10}$$

where $\hat{F}^j$ (like $\hat{u}$) is gauge invariant, Σ the (planar) surface bound by the curve C_s, and $d\Sigma$ an element of area on that surface. Where $\hat{u}$ is not differentiable, we will have to break this integral into a surface integral over the region where $\hat{u}$ is analytic, and line integrals surrounding each of the non-analyticities in $\hat{u}$. We shall concentrate on the contribution from these non-analyticities below.

Through this choice of θ, we have suggested that the dynamics describing confinement can be expressed in terms of only an Abelian field, and the suggestion and feasibility of using this choice of θ as the basis of a CDG decomposition is the most important novelty and result of this work. The coloured part of the gauge field, X_μ, does not contribute to confinement. We do not require any additional path integrals. This procedure is gauge invariant, in the sense that θ transforms gauge covariantly, and therefore the restricted field strength $\hat{F}_{\mu\nu}$ and all other observables constructed from the restricted field $\hat{A}$ are gauge invariant.

3. Topological structures

Now suppose that $\hat{u}^j$ contains a non-analyticity. We integrate the field around a loop $\tilde{C}$ parametrised by $\tilde{\sigma}$ surrounding the discontinuity in $\hat{u}^j$, bounding the surface integral by an additional line integral $\oint_{\tilde{C}} d\tilde{\sigma}\,\hat{u}_{\tilde{\sigma}}^j$. We define $\{\tilde{C}_n\}$ as the set of curves surrounding all these discontinuities, and $\tilde{\Sigma}$ the area bound within these curves. Thus

$$e^{i\lambda^j\delta\tilde{\sigma}\hat{u}_{\mu,x}^j} = \theta_x^\dagger\hat{X}_{\mu,x}^\dagger\theta_x\theta_x^\dagger U_{\mu,x}\theta_{x+\delta\tilde{\sigma}}, \tag{11}$$

---

[2] The proof that this can be done for each link on a Wilson loop is straightforward, and shall be provided in the follow-up article.

and $\hat{u}_{\mu,x}^j$ is continuous on $\tilde{C}$. After gauge-fixing, we expand $U_\mu = 1 - i\frac{1}{2}g\delta\tilde{\sigma}A_\mu^a\lambda^a$ and $\theta_x^\dagger\theta_{x+\delta\tilde{\sigma}} = 1 + \delta\tilde{\sigma}\theta_x^\dagger\partial_{\tilde{\sigma}}\theta_x$. We assume that $X_0 \equiv \frac{1}{2}\theta_x^\dagger(\hat{X}_{\mu,x} + \hat{X}_{\mu,x}^\dagger)\theta_x$, which will be close to the identity operator, is well-defined along $\tilde{C}$.

$$
\begin{aligned}
i\delta\tilde{\sigma}\hat{u}_{\mu,x}^j &= \frac{1}{\mathrm{tr}(\lambda^j)^2}\mathrm{Im}\big(\mathrm{tr}\big[\lambda^j\theta_x^\dagger\hat{X}_{\mu,x}^\dagger\theta_x\theta_x^\dagger U_{\mu,x}\theta_{x+\delta\tilde{\sigma}\hat{\mu}}\big]\big) \\
&= \frac{1}{2\mathrm{tr}(\lambda^j)^2}\mathrm{tr}\big[\lambda^j\theta_x^\dagger\big(\hat{X}_{\mu,x}^\dagger - \hat{X}_{\mu,x}\big)\theta_x \\
&\quad - i\lambda^j\delta\tilde{\sigma}\theta_x^\dagger[X_0]_{\mu,x}gA_{\mu,x}^a\lambda^a\theta_x \\
&\quad + 2\lambda^j\theta^\dagger[X_0]_{\mu,x}\theta_x\delta\tilde{\sigma}\theta_x^\dagger\partial_{\tilde{\sigma}}\theta\big].
\end{aligned}
\tag{12}
$$

Using (8), if A_μ and X_0 are analytic the final term with a derivative in θ will dominate, giving

$$
\begin{aligned}
\theta_s^\dagger W[C_s]\theta_s = \exp\bigg(i\lambda^j\bigg[&\int\limits_{(x\in\Sigma)\cap(x\notin\tilde{\Sigma})} d\Sigma_{\mu\nu}\,\hat{F}_{\mu\nu}^j \\
&+ \sum_n\oint\limits_{\tilde{C}_n} d\tilde{\sigma}\,\frac{1}{\mathrm{tr}(\lambda^j)^2}\mathrm{tr}\big[\lambda^j X_0\theta^\dagger\partial_{\tilde{\sigma}}\theta\big]\bigg]\bigg).
\end{aligned}
\tag{13}
$$

There are three occasions when θ (and thus $\hat{u}$) may be discontinuous: if the Wilson loop has degenerate eigenvalues; if the gauge field A_μ is discontinuous; but we will here concentrate on the possibility described below, which occurs in locations where A_μ is analytic [35].

In SU(2), we parametrise θ as

$$
\theta = (\cos a\,\mathbb{I} + i\sin a\,\phi)e^{id_3\lambda^3}, \qquad \phi = \begin{pmatrix} 0 & e^{ic} \\ e^{-ic} & 0 \end{pmatrix},
$$

$$
\bar{\phi} = \begin{pmatrix} 0 & ie^{ic} \\ -ie^{-ic} & 0 \end{pmatrix}, \qquad \lambda^3 = \begin{pmatrix} 1 & 0 \\ 0 & -1 \end{pmatrix},
\tag{14}
$$

with $c\in\mathbb{R}$ and $0 \leqslant a \leqslant \pi/2$. $d_3\in\mathbb{R}$ is determined by the fixing condition. $\mathbb{I}$ is the identity operator. As θ contains the eigenvectors of $W[C_s]$, it is differentiable except where $W[C_s]$ has degenerate eigenvalues and those points at $a = 0$ or $a \approx \pi/2$ where c is ill-defined. We parametrise the plane of the Wilson loop using polar coordinates (r, ψ), with $r = 0$ at $a = \pi/2$. At infinitesimal but non-zero r, $c(r, \psi = 0) = c(r, \psi = 2\pi) + 2\pi\nu_n$ for integer winding number ν_n. With c ill-defined at $r = 0$, we may find that $\nu_n \neq 0$. This will lead to the emergence of structures in $\hat{F}$ with a large field strength. a and c are not gauge invariant, so the corresponding structures in the gauge invariant $\hat{F}$ will be extended over a region rather than just a single point. This means that when we integrate the gauge invariant $\hat{u}$ along a curve around the singularity we should not choose the curve precisely at $a = \pi/2$, but some other path which both respects gauge invariance and contains the singularities in all gauges. We could, perhaps, use loops of non-vanishing magnetic current $k_\mu = \frac{1}{2}\epsilon_{\mu\nu\rho\sigma}\partial^\nu F^{\rho\sigma}$ to define this path (cf. [30] and its references for a discussion of these loops), but, for simplicity, we have here assumed that we can construct a suitable curve at some constant $a = a_0$; while other choices might be better, they will not make any significant difference to our conclusions. It is straightforward to calculate

$$
\begin{aligned}
\theta^\dagger\partial_\sigma\theta = e^{-id_3\lambda^3}\big[&i\partial_\sigma a\phi + i\lambda^3\partial_\sigma d \\
&+ i\sin a\cos a\bar{\phi}\partial_\sigma c - i\sin^2 a\partial_\sigma c\lambda^3\big]e^{id_3\lambda^3}.
\end{aligned}
\tag{15}
$$

We integrate along a path at fixed a surrounding the structure in $\hat{F}$, with a fixing condition holding d_3 constant,

$$
\begin{aligned}
\theta_s^\dagger W[C_s]\theta_s &= e^{i\lambda^3[\int_{(x\in\Sigma)\cap(x\notin\tilde{\Sigma})} d\Sigma_{\mu\nu}\,\hat{F}_{\mu\nu}^j - \sum_n\oint_{\tilde{C}_n} d\tilde{\sigma}\,\partial_{\tilde{\sigma}}c\sin^2 a_{0n}]} \\
&= e^{i\lambda^3[\int_{(x\in\Sigma)\cap(x\notin\tilde{\Sigma})} d\Sigma_{\mu\nu}\,\hat{F}_{\mu\nu}^j - \sum_n 2\pi\nu_n\lambda^3\sin^2 a_{0n}]}.
\end{aligned}
\tag{16}
$$

If $\nu_n \neq 0$ the structures arising from this discontinuity give a significant contribution to the restricted field strength. The total Wilson loop will be the product of a perimeter term, any remaining area law contribution from the surface integral over $\hat{F}_{xt}$, and contributions from all these structures. As we can expect the number of structures to be proportional to the area of the loop, this leads to an area law for the Wilson loop and a linear string tension.

Although $\hat{F}$ (and therefore the structures) is gauge-invariant, θ, $\hat{X}$ and $\hat{U}$ depend on the gauge. Since we require that the gauge field is continuous, we can only use continuous gauge transformations. However, to undo the winding in θ requires a discontinuous gauge transformation. Thus the discontinuities in θ will survive any smooth gauge transformation. For example, in SU(2), we can parametrise an infinitesimal gauge transformation as

$$
\Lambda = \begin{pmatrix} \cos l_1 & i\sin l_1 e^{il_2} \\ i\sin l_1 e^{-il_2} & \cos l_1 \end{pmatrix}\begin{pmatrix} e^{il_3} & 0 \\ 0 & e^{-il_3} \end{pmatrix},
\tag{17}
$$

with l_1 and l_3 infinitesimal and analytic and $0 < l_2 < 2\pi$. If we fix $d_3 = 0$, we find that for $|a| \gg O(l_1, l_3)$ and $|\pi/2 - a| \gg O(l_1, l_3)$,

$$
\begin{aligned}
c &\to c' = c + 2l_3 + l_1\sin(l_2 - c)\cot a - l_1\sin(l_2 - c)\tan a, \\
a &\to a' = a + l_1\frac{\cos(l_2 - c)}{\cos a}.
\end{aligned}
\tag{18}
$$

The winding number becomes

$$
\nu \to \oint \partial_{\tilde{\sigma}}c'd\tilde{\sigma} = \oint \partial_{\tilde{\sigma}}(c' - c)d\tilde{\sigma} + 2\pi\nu,
\tag{19}
$$

and since l_1 and l_3 are infinitesimals and cannot change by 2π and $(c' - c)$ is invariant under $c \to c + 2\pi\nu$, the winding number is unaffected. The location where $a = \pi/2$ or 0 may, however, be shifted by a small amount.

In a SU(N_C) gauge theory, we parametrise θ in terms of $N_C - 1$ diagonal elements $e^{id_j\lambda^j}$ and $(N_C^2 - N_C)/2$ matrices $e^{ia_i\phi_i} \in$ SU(2)/U(1), with each ϕ_i a different embedding of Eq. (14) into su(N_C) [35]. Since the different ϕ_i do not commute, this parametrisation is not unique; nonetheless once the parametrisation is fixed the analysis proceeds as in SU(2), and the winding number is independent of the choice of parametrisation. There will be a peak in $\hat{F}_{\mu\nu}$ whenever a c_i winds around a point where $a_i = \pi/2$ for any of the SU(2)/U(1) matrices, and each of those peaks contributes to the string tension.

4. Numerical results

We generated $16^3 \times 32$ and $20^3 \times 40$ quenched lattice QCD (SU(3)) configurations with a Tadpole Improved Luscher–Weisz gauge action [31] using a Hybrid Monte Carlo routine [32] (see Table 1). The lattice spacing was measured using the string tension $\rho \sim (420\text{ MeV})^2$. We applied ten steps of improved stout smearing [33,34] with parameters $\rho_s = 0.015$ and $\epsilon = 0$. θ and $\hat{U}$ were extracted from the gauge field by solving equations (5), (7) and (8) numerically. Our algorithms and numerical set-up will be fully described in a subsequent publication.

To match the continuum calculations, we need to work in a continuous gauge, which is difficult to realise on the lattice. We have therefore only used gauge-invariant observables here, the string tension and restricted field strength. Extracting the components a and c from the gauge-dependent θ is straightforward: we presented some results for the winding of c around the peaks in [27]. However, it is unclear what physical meaning can be given

Table 1
Parameters for our simulations: the lattice size, the spatial extent of the lattice, L, the inverse gauge coupling β, the lattice spacing a, and the number of configurations in each ensemble #.

Lattice size	L (fm)	β	a (fm)	#
$16^3 \times 32$	2.30	8.0	0.144(2)	91
$16^3 \times 32$	1.84	8.3	0.114(1)	91
$16^3 \times 32$	1.58	8.52	0.099(1)	82
$20^3 \times 40$	2.30	8.3	0.112(5)	61

to this as we will be in a different gauge to the continuum calculations.

The string tension from the restricted potential is gauge invariant, and can be extracted from the Wilson loop in a standard way. The restricted field strength can be measured using the gauge-invariant plaquette definition

$$e^{\hat{F}_{xt}^j(x+\frac{1}{2}a,t+\frac{1}{2}a)\lambda^j}$$
$$\sim \theta_x^\dagger \hat{U}_x(x,t)\hat{U}_t(x+a,t)\hat{U}_x^\dagger(x,t+a)\hat{U}_t^\dagger(x,t)\theta_x. \quad (20)$$

Constructing the θ contribution to the restricted field strength is more challenging because the direct calculation, measuring $\mathrm{tr}\lambda^j(\theta_x^\dagger\theta_{x+a\hat\mu}-1) \sim \mathrm{tr}\lambda^j(\theta_{x+\frac{1}{2}a\hat\mu}^\dagger\partial_\mu\theta_{x+\frac{1}{2}a\hat\mu})$ for lattice spacing a, is not gauge-invariant. A gauge transformation which would be discontinuous in the continuum could lead to additional discontinuities appearing in the observable or the removal of discontinuities already present. Fixing the gauge does not help, as we might fix to a gauge where A_μ is discontinuous. We need to instead study the quantity $\theta_x^\dagger \tilde{U}_{x,\mu}\theta_{x+\hat\mu}$ for some gauge covariant field $\tilde{U}$ (so the whole expression is gauge-invariant) which has only a minor effect on physical observables such as the string tension so that only θ contributes to the Wilson loop (the operator we use to represent $\tilde{U}$ is given later).

Stout smearing [33,34] is a well-known tool to smooth the gauge field while preserving gauge invariance. Each Stout smearing sweep replaces $U_{x,\mu} \rightarrow U_{x,\mu}' = e^{iQ_x}U_{x,\mu}$ where Q is a Hermitian operator constructed from closed loops of gauge links starting and finishing at x (we constructed Q from plaquettes and 2×1 rectangles [34]). A few smearing sweeps are often used to remove unwanted discontinuous fluctuations in the gauge field. Too many smearing steps risk destroying the physical features of the gauge field. This is what we require: we set $\tilde{U}$ to be the gauge field U subjected to a large number of stout smears: $\tilde{U}$ should resemble a pure gauge transformation, as any closed loop of gauge links will give the identity operator and thus a zero field strength. We perform an Abelian decomposition on $\theta_x^\dagger\tilde{U}_{x,\mu}\theta_{x+\hat\mu}$ to extract the restricted field $\hat{\tilde{U}}_{x,\mu}$ which satisfies $[\hat{\tilde{U}}_{x,\mu},\lambda^j]=0$ and $\mathrm{tr}(\lambda^j(\tilde{X}-\tilde{X}^\dagger))=0$ with $\tilde{X}=\theta_x^\dagger\tilde{U}_{x,\mu}\theta_{x+\hat\mu}(\hat{\tilde{U}}_{x,\mu})^{-1}$. We compare the field strength from this $\hat{\tilde{U}}$, representing the θ contribution to the restricted field strength, to the field strength from the restricted field $\hat{U}$. We expect that the observables calculated from the θ field and the restricted field should be similar: the string tensions should be similar, and the field strengths should contain similar features.

In Fig. 1 and Table 2, we extract the string tension, ρ, for the original gauge field U, the restricted field $\hat{U}$ and the θ contribution to the restricted field, $\hat{\tilde{U}}$. We have calculated the expectation value of the $R\times T$ Wilson loop in the xt plane for one of the fields, and fit it to the function $\rho RT + aR + bT + c + dR/T + eT/R + f/T + g/R + h/(TR)$ for unknown coefficients $\rho, a, \ldots, h$. The cited errors are statistical, calculated using the bootstrap method, and systematic, reflecting uncertainties in the fitting. To reduce the computa-
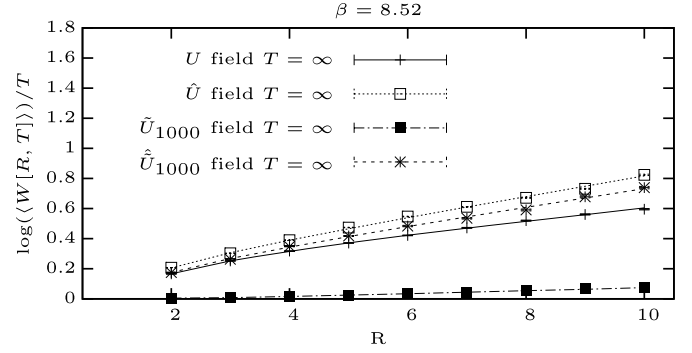

Fig. 1. The string tension extrapolated to infinite time for the original gauge field U, the restricted gauge field $\hat{U}$, the over-smeared field $\tilde{U}$ and the θ contribution to $\hat{U}$, $\hat{\tilde{U}}$, for a $\beta = 8.52$ ensemble.

Table 2
The string tension extrapolated to infinite time across all our ensembles. 8.3L refers to the $20^3 \times 40$ ensemble. The last two rows give the ratio of the topological and restricted string tensions and the restricted and actual string tensions.

β	8.0	8.3	8.52	8.3L
U	0.094(2)	0.064(3)	0.041(1)	0.059(1)
$\hat{U}$	0.106(4)	0.087(2)	0.072(1)	0.095(1)
$\tilde{U}_{100}$	0.0835(4)	0.0536(3)	0.0413(3)	0.0554(3)
$\hat{\tilde{U}}_{100}$	0.111(5)	0.080(2)	0.071(2)	0.093(2)
$\tilde{U}_{300}$	0.0465(2)	0.0297(2)	0.0231(3)	0.0295(2)
$\hat{\tilde{U}}_{300}$	0.099(5)	0.079(2)	0.068(2)	0.091(2)
$\tilde{U}_{500}$	0.0317(2)	0.0214(1)	0.0168(2)	0.0207(2)
$\hat{\tilde{U}}_{500}$	0.096(5)	0.080(2)	0.067(2)	0.096(1)
$\tilde{U}_{600}$	0.0273(2)	0.0187(1)	0.0148(2)	0.0178(1)
$\hat{\tilde{U}}_{600}$	0.094(5)	0.080(2)	0.067(2)	0.093(1)
$\tilde{U}_{800}$	0.0212(2)	0.0150(1)	0.0121(2)	0.0142(1)
$\hat{\tilde{U}}_{800}$	0.093(7)	0.080(2)	0.068(2)	0.092(2)
$\tilde{U}_{1000}$	0.0173(2)	0.0123(1)	0.0103(2)	0.0119(1)
$\hat{\tilde{U}}_{1000}$	0.093(7)	0.080(2)	0.068(2)	0.092(2)
$\frac{\hat{\tilde{U}}_{1000}}{\hat{U}}$	0.88(7)	0.92(3)	0.94(3)	0.97(2)
$\frac{U}{\hat{U}}$	0.89(4)	0.74(4)	0.57(2)	0.62(1)

tional overhead, for this initial study we did not recalculate a new θ field for each Wilson loop but reused the same θ field for our whole configuration, a simplification which destroys the identity between the Wilson loops for the U and $\hat{U}$ fields; but is likely to keep any correlation between the $\hat{\tilde{U}}$ and $\hat{U}$ fields intact. We are currently in the process of calculating the string tension with θ recalculated for each Wilson loop, and intend to present the updated result in a follow-up publication (early results are mentioned in [28]). We do not expect that the string tension between the U and $\hat{U}$ fields will be identical, and, indeed, there is a large discrepancy in our results (which increases with decreasing lattice spacing). This would be particularly true for Wilson loops not on the xt plane (we have broken the hypercubic symmetry of the lattice by singling out the xt plane while constructing θ), so we have here restricted our study to Wilson loops in the xt plane. In this work, we are therefore more interested in the relationship between the string tension extracted from $\hat{\tilde{U}}$ and $\hat{U}$. Were these closely related, it would suggest that the topological (θ) contribution to the string tension dominates, which is likely to be replicated in the full calculation where the string tensions for $\hat{U}$ and U will be identical.

We calculate $\tilde{U}$ after 100, 300, 500, 600, 800 and 1000 sweeps of stout smearing with parameters $\epsilon = 0$, $\rho_s = 0.1$ (following [34]). We also show the string tension for $\tilde{U}$, and can confirm that it is
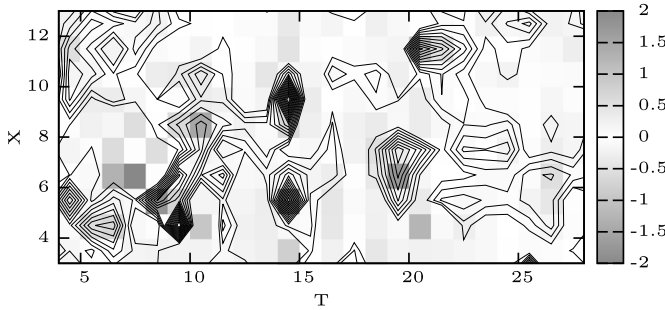
Fig. 2. A comparison between the peaks in $\hat{F}_{xt}^3$ (contours) against the topological field strength extracted from $\hat{U}$ (shaded background). In this presentation the negative and positive peaks cannot be distinguished. We show one (typical) slice of the lattice at $Y = 0$, $Z = 11$. Due to the limited resolution of the lattice, the extrapolated contour lines and the shading have an error of up to one lattice spacing.

Fig. 3. The $\hat{U}$ string tension, ρ, excluding Wilson loops containing peaks of height $|F_{xt}| > \mathcal{K}$ from the average ($\beta = 8.52$ ensemble).

Table 3
The $\hat{U}$ string tension, ρ (in units of $10^{-2}a^{-1}$), excluding Wilson loops containing peaks of height $|F_{xt}| > \mathcal{K}$ from the average ($\beta = 8.52$ ensemble). $\beta 8.3L$ refers to the $20^3 40$ ensemble.

$\mathcal{K}$	2.55	1.30	1.05	0.55	0.30
$\beta 8.0$	12.1(5)	12.0(4)	11.5(3)	10.3(4)	5.00(1)
$\beta 8.3$	9.2(1)	9.0(1)	8.8(1)	7.7(1)	3.82(1)
$\beta 8.52$	7.7(1)	7.8(1)	7.6(1)	6.7(1)	5.0(3)
$\beta 8.3L$	9.8(1)	9.0(1)	8.4(1)	7.3(1)	4.56(7)

much smaller than that of the original gauge field and decreases as we increase the level of smearing. The string tension for $\hat{U}$ is unaffected by sufficiently large amounts of smearing, suggesting that we have indeed measured the contribution from $\theta\partial_\mu\theta^\dagger$ rather than any remnant of U remaining after the smearing.

There is a considerable difference between the string tension for the original gauge field and for the restricted and topological fields, and this seems to increase as the lattice spacing decreases (the $\beta = 8.0$ 16^3 ensemble and 20^3 ensemble have roughly the same physical volume at different lattice spacings). The difference becomes very pronounced on the $\beta = 8.52$ ensemble. The $\hat{U}$ string tension has a weaker dependence on β than that calculated from the actual gauge field. This is an artefact of the approximation we have made to accelerate the calculation, and both the approximation and its artefact will be removed in future work. Of more interest is the difference between the topological and restricted string tension, more likely to be duplicated in the calculation after our approximation has been removed. We see that the topological string tension appears to be slightly lower than the restricted tension on all our ensembles, by about 2σ or 88–97%. The variation of this discrepancy across our ensembles is not statistically significant. In all our ensembles the topological part of the restricted field dominates the restricted string tension.

Is the restricted field strength dominated by the expected peaks? We use a contour plot to display the distribution of $\hat{F}_{xt}^3$ in Fig. 2 on a slices of the lattice. The results for $\hat{F}_{xt}^8$ are similar. $\hat{F}_{xt}^3$ is indeed dominated by objects one or two lattice spacings across. There is no correlation with the structures on the neighbouring lattice slices, indicating that these are point like objects rather than strings or surfaces. Do these peaks emerge from the θ field? The background shading of Fig. 2 shows the topological ($\hat{U}$) field strength, and there is a strong correspondence between the location of the peaks in these two fields (albeit sometimes shifted by a lattice spacing – the resolution of our operators, and a few structures visible in the topological field strength but not $\hat{F}_{xt}$). This pattern is repeated across all our ensembles.

We next investigate whether these peaks are responsible for the string tension. Does excluding these peaks reduce or eliminate the confining potential? We usually measure the expectation value of the Wilson loop by averaging over every planar loop in the configuration (in the xt plane). Here we only include loops which do not contain peaks higher than a cut-off $|\hat{F}| > \mathcal{K}$, excluding those Wilson loops which contain one of the peaks from the average. In Fig. 3 and Table 3, we see that the string tension gradually decreases when averaging only over those loops with $|F| < 1.0$ – as expected if the peaks rather than the fluctuations around zero are
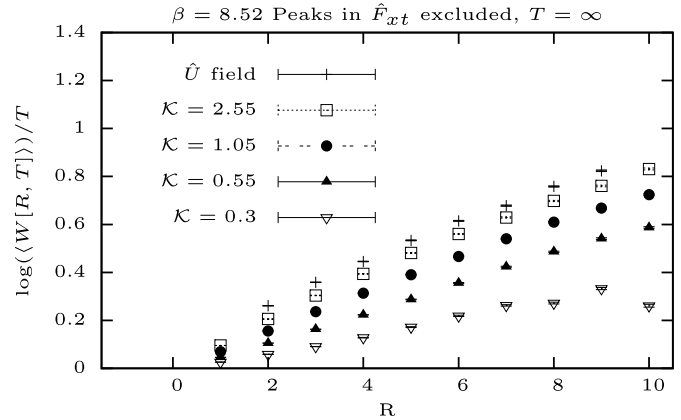
responsible for the confining string. This pattern is again duplicated across our ensembles.

5. Conclusions

We have proposed a method to express the Wilson loop of a non-Abelian field in terms of an Abelian field without gauge fixing. Implementing the gauge invariant Abelian decomposition (the CDG decomposition) on the lattice we relate the Wilson loop to a surface integral over the CDG decomposition's restricted potential, and show that the restricted potential leads to an area law scaling for the quark–quark potential, and thus confinement. This confirms Abelian dominance of confinement.

The restricted potential contains two terms, one from the original gauge field (the naive Abelian part) and the other from the derivative of the θ field (the topological part). To isolate the cause of confinement, we must show which of these parts is most important for confinement. In this Letter we have given evidence suggesting that the topological part dominates the Wilson loop integral, and thus confines the colour. This strongly endorses the recent Chiba-KEK lattice calculations [22,23].

The Wilson loop describes the chromoelectric flux between quarks. While the topological part of the restricted gauge potential is known to contain coloured monopoles [16,17], so our lattice simulations are consistent with the recent theoretical analysis showing that monopole condensation generates confinement [8], in this work we have only demonstrated that the topological potential is responsible for the area law of the Wilson loop. The structures we have found in the this component of the field strength are points rather than lines, suggesting that there is something else occurring (an isolated Wang–Yu monopole should have no contribution to the component of the field strength, $\hat{F}_{xt}$, studied here [35]). The structures found in the electric field are certainly not isolated monopoles. More work is needed to compare our results with various models of the vacuum and see whether these objects are caused by monopole condensation or some other mechanism.

Another important open question is how much the structures we have found in the restricted field will also be present in the restricted fields constructed from a different choice of θ (for example, by using a different set of nested Wilson loops). If the structures are unique to this choice of θ, then their use in identifying topological structures in the QCD vacuum causing confinement will be limited. However, since the gauge field strength $F_{\mu\nu}[A]$ can be decomposed as $F_{\mu\nu} = \hat{F}_{\mu\nu} + F[X]_{\mu\nu} - ig([\hat{A}_\mu, X_\mu] - [\hat{A}_\nu, X_\nu])$, where X_μ does not contribute to confinement, we hypothesise that many structures found in $\hat{F}$ will be present in F; and that many structures leading to confinement contained within F might be present in the $\hat{F}$ constructed from diverse choices of θ. However, this hypothesis should be either confirmed or falsified in a future numerical study.

Furthermore, we should also study the directional dependence of the field strength (and the Wilson loop). In subsequent studies [28,35], we will consider the other components of the field strength tensor, finding that here the structures manifest themselves as one dimensional strings as well as points. In view of these later results, it is likely that the string tension will be larger if measured off the xt plane. This discrepancy is only an artefact of our approximation, using the same θ for each Wilson loop, and will be absent in a calculation without this simplification.

Our work is ongoing, and a full description of our theory and methods, and expanded numerical results, will be given in due course [35].

Acknowledgements

References

[1] G. 't Hooft, in: A. Zichichi (Ed.), High Energy Physics, Editrice Comprostrini, Bologna, 1976.
[2] G. 't Hooft, Nucl. Phys. B 190 (1981) 455.
[3] Y. Nambu, Phys. Rev. D 10 (1974) 4262.
[4] G. 't Hooft, Nucl. Phys. B 79 (1974) 276.
[5] A.M. Polyakov, JETP Lett. 20 (1974) 194.
[6] S. Mandelstam, Phys. Rep. 23C (1976) 245.
[7] A. Polyakov, Nucl. Phys. B 120 (1977) 429.
[8] Y.M. Cho, Dimensional transmutation by monopole condensation in QCD, Phys. Rev. D 87 (2013) 085025, arXiv:1206.6936.
[9] Y.M. Cho, Abelian dominance in Wilson loops, Phys. Rev. D 62 (2000) 074009, http://dx.doi.org/10.1103/PhysRevD.62.074009, arXiv:hep-th/9905127.
[10] A. Kronfeld, M. Laursen, G. Schierholz, U.-J. Wiese, Monopole condensation and color confinement, Phys. Lett. B 198 (4) (1987) 516–520, http://dx.doi.org/10.1016/0370-2693(87)90910-5.
[11] T. Suzuki, I. Yotsuyanagi, A possible evidence for Abelian dominance in quark confinement, Phys. Rev. D 42 (1990) 4257–4260, http://dx.doi.org/10.1103/PhysRevD.42.4257.
[12] J.D. Stack, S.D. Neiman, R.J. Wensley, String tension from monopoles in SU(2) lattice gauge theory, Phys. Rev. D 50 (1994) 3399–3405, http://dx.doi.org/10.1103/PhysRevD.50.3399, arXiv:hep-lat/9404014.
[13] H. Shiba, T. Suzuki, Monopole action and condensation in SU(2) QCD, Phys. Lett. B 351 (1995) 519–527, http://dx.doi.org/10.1016/0370-2693(95)00422-H, arXiv:hep-lat/9408004.
[14] N. Arasaki, S. Ejiri, S.-i. Kitahara, Y. Matsubara, T. Suzuki, Monopole action and monopole condensation in SU(3) lattice QCD, Phys. Lett. B 395 (1997) 275–282, http://dx.doi.org/10.1016/S0370-2693(97)00066-X, arXiv:hep-lat/9608129.
[15] P. Cea, L. Cosmai, Abelian monopole and vortex condensation in lattice gauge theories, J. High Energy Phys. 0111 (2001) 064.
[16] Y.M. Cho, Phys. Rev. D 21 (1980) 1080.
[17] Y.M. Cho, Phys. Rev. D 23 (1981) 2415.
[18] Y. Duan, M. Ge, Sci. Sin. 11 (1979) 1072.
[19] L. Faddeev, A. Niemi, Phys. Rev. Lett. 82 (1999) 1624, arXiv:hep-th/9807069.
[20] S. Shabanov, Phys. Lett. B 458 (1999) 322, arXiv:hep-th/9903223.
[21] T.T. Wu, C.N. Yang, in: H. Mark, S. Fernbach (Eds.), Properties of Matter under Unusual Conditions, Interscience, New York, 1969.
[22] K.-I. Kondo, T. Murakami, T. Shinohara, Yang–Mills theory constructed from Cho–Faddeev–Niemi decomposition, Prog. Theor. Phys. 115 (2006) 201–216, http://dx.doi.org/10.1143/PTP.115.201, arXiv:hep-th/0504107.
[23] K.-I. Kondo, A. Shibata, T. Shinohara, S. Kato, Non-abelian dual superconductor picture for quark confinement, Phys. Rev. D 83 (2011) 114016, http://dx.doi.org/10.1103/PhysRevD.83.114016, arXiv:1007.2696.
[24] A. Shibata, et al., Toward gauge independent study of confinement in SU(3) Yang–Mills theory, PoS LATTICE 2007 (2007) 331, arXiv:0710.3221.
[25] D. Diakonov, V.Y. Petrov, A formula for the Wilson loop, Phys. Lett. B 224 (1989) 131–135, http://dx.doi.org/10.1016/0370-2693(89)91062-9.
[26] D. Diakonov, V.Y. Petrov, Generating functional for Yang–Mills theory and the confinement requirement, Phys. Lett. B 242 (1990) 425–428, http://dx.doi.org/10.1016/0370-2693(90)91787-C.
[27] N. Cundy, W. Lee, J. Leem, Y. Cho, String tension from gauge invariant magnetic monopoles, PoS LATTICE 2012 (2012) 213, arXiv:1211.0664.
[28] N. Cundy, Y. Cho, W. Lee, The gauge invariant abelian decomposition, PoS LATTICE 2013 (2013) 471, arXiv:1311.3029.
[29] K.G. Wilson, in: M. Levy, P. Mitter (Eds.), New Developments in Quantum Field Theory and Statistical Mechanics, Plenum, New York, 1977.
[30] A. Shibata, et al., Topological configurations of Yang–Mills field responsible for magnetic-monopole loops as quark confiner, PoS LATTICE 2009 (2009) 232, arXiv:0911.4533.
[31] M. Lüscher, P. Weisz, Commun. Math. Phys. 97 (1985) 59.
[32] S. Duane, A. Kennedy, B. Pendleton, D. Roweth, Phys. Lett. B 195 (1987) 216.
[33] C. Morningstar, M.J. Peardon, Phys. Rev. D 69 (2004) 054501, arXiv:hep-lat/0311018.
[34] P.J. Moran, D.B. Leinweber, Phys. Rev. D 77 (2008) 094501, http://dx.doi.org/10.1103/PhysRevD.77.094501, arXiv:0801.1165.
[35] N. Cundy, Y.M. Cho, W. Lee, in preparation.